

## **A CASE OF SEVERE ELEVATED CONVECTION OVER THE OHIO VALLEY ON MARCH 22-23, 1995**

*Kevin J. Farina  
and  
John T. DiStefano  
NOAA/National Weather Service Office  
Wilmington, Ohio*

### **1. INTRODUCTION**

Elevated convection is difficult to forecast considering the fact that the convection usually occurs above a stable boundary layer. In the Ohio Valley, convection that occurs during the cold season is generally elevated in nature. Colman (1990a and 1990b) has laid the groundwork for studies on elevated convection by identifying the climatology, organization, and instability mechanisms involved in the development of thunderstorms above a stable boundary layer.

According to Colman (1984 and 1990a), elevated thunderstorms are defined as those storms occurring above frontal surfaces, isolated from surface diabatic effects. His research found that elevated thunderstorms frequently occur in environments exhibiting negative Convective Available Potential Energy (CAPE). He also found that these elevated thunderstorms generally occur northeast of the surface low pressure system, and north of a surface warm front in a region of very stable air in the boundary layer. This type of convection occurs in a strong low level wind shear environment ahead of the low and mid level jet streaks. He also observed that elevated convection develops as

high theta-e air moves over a surface warm front in a strongly baroclinic environment.

This paper describes, in some detail, a case of severe elevated convection that occurred over the Ohio Valley on March 22-23, 1995, with a focus on the environment in which the thunderstorms occurred. Comparisons are made between this event and the findings from Colman (1984, 1990a, and 1990b). Section 2 describes the data used in this study, while section 3 reviews the climatology of elevated convection. Section 4 presents the synoptic overview from both the dynamic and thermodynamic perspectives, and section 5 discusses radar observations during the event. Lastly, section 6 presents a summary.

### **2. DATA**

Surface and upper air data (850, 700, 500 and 300 mb) from 0000 and 1200 UTC on March 23, 1995 were obtained from the National Climate Data Center. Sounding data from Dayton, Ohio, as well as NGM and ETA gridded data were also obtained. The SkewT/Hodograph Analysis and Research Program (Hart and Korotky 1991) was used to analyze and modify the sounding data, while

the NWS PC-based GRidded Information Display and Diagnosis System (PCGRIDDS) was utilized to diagnose the model grids. In addition, infrared satellite imagery were obtained from the National Environmental Satellite, Data and Information Service (NESDIS) for the period 1800 UTC on March 22 through 1200 UTC on March 23, 1996. Archive IV data (FMH-11; Part A, 1991) from the Wilmington, Ohio WSR-88D (KILN) was also obtained for the overnight period of March 22-23.

### **3. CLIMATOLOGY**

The Wilmington, Ohio, county warning area receives more elevated convection on average than any point longitudinally east of the area (Colman 1990a). The peak time for elevated convection is during the spring months of March and April when the upper atmosphere is generally colder and when the boundary layer can rapidly heat and be lifted over a frontal boundary.

### **4. SYNOPTIC OVERVIEW**

#### **a. Dynamic Environment**

Colman (1990a) found that elevated thunderstorms generally occur in the sector north and northeast of the surface low. He also noted that 46% of events he researched were associated with warm fronts, where the median distance from the thunderstorm to the front was 1.9 degrees of latitude ( $\approx 115$  nm).

The convection on March 23 developed northeast of a surface low that was forecast to track from the Kansas/Missouri border to the Missouri Bootheel between 0000 and 0600 UTC (Figs. 1a and 1b). At 0000 UTC, a

warm front was observed extending east-southeast from the low into Tennessee, and was forecast to be positioned across the Carolinas by 1200 UTC. The severe convection developed in southeast Indiana and north-central Kentucky, approximately 1.6 degrees ( $\approx 95$  nm) north of the front and northeast of the surface low; favorable areas according to Colman.

Colman (1990a) also found that elevated thunderstorms occur in environments exhibiting extreme directional wind shear between the surface and 850 mb (generally surface winds northeast to southeast and 850-mb winds south to southwest). The severe thunderstorm activity in this study also formed in a similar type environment with surface and 850-mb winds from the east and southwest, respectively (see Fig. 2). In addition, Colman found that elevated convection occurred in strong 850-mb warm advection, in cyclonically curved flow and downstream of the low level jet. Figure 3 shows the elevated thunderstorms on March 23 occurred in a similar environment.

Also in concurrence with Colman's observations, this area of elevated thunderstorm activity was observed to have developed close to, or slightly downstream from the inflection point in the 500-mb flow pattern. Trough alignment was such that positive differential vorticity advection with height was clearly identified in selected vertical time-height profiles taken from this convective development region. This forcing, coupled with the indicated warm air advection pattern, aided in the resultant deep upward vertical motion that was evident around 0600 UTC in the model gridded data fields. In addition, Colman noted that the 850 mb level usually possesses the highest theta-e air and is most likely the source region for elevated

convection. At 0000 UTC on March 23, the strongest 850-mb theta-e advection was over Illinois (not shown), where the elevated convection developed. By 0600 UTC, the strongest theta-e advection was forecast across Indiana and Kentucky (Fig. 4).

Colman also observed that winds between the 850 and 500 mb levels generally exhibited both veering and increasing speed with height over the area experiencing elevated convection. This pattern was mirrored in the 0600 UTC ETA forecasted model gridded data where winds veered similarly with height and increased in speed from around 20 kts at 850 mb to between 45-50 kts at 500 mb over the Ohio Valley (Fig. 5). The VAD Wind Profile from the Wilmington, Ohio WSR-88D around 0500 UTC also identified this 850-500 mb layer shear pattern (not shown).

According to Colman, the location of elevated convection relative to associated 850-mb and 500-mb wind maximum was situated primarily in the left-front (39%) and right-front (37%) quadrants, respectively. The elevated convection that occurred on March 23 in the Ohio Valley lined up rather well with this finding (Figs. 6a and 6b).

Infrared (IR) satellite imagery depicted the convection north of the surface warm front. Specifically, the IR image at 0015 UTC on March 23 showed enhanced cloud tops along and just to the north of the warm front in Kentucky. At this time, storms were developing over central Illinois (Fig. 7). These storms moved out of Illinois and tracked southeastward across Indiana between 0200 and 0500 UTC. By the time the storms reached northeastern Kentucky (around 0645 UTC), cloud top temperatures had warmed somewhat (Fig. 8).

## **b. Thermodynamic Environment (Stability Analysis)**

Stability indices reveal the potential buoyancy of an air parcel. One example is the surface-based Lifted Index (LI). Here, a parcel is lifted dry adiabatically from the surface to its Lifted Condensation Level (LCL), and then moist adiabatically to 500 mb where the parcel temperature is compared to its environmental temperature. The Showalter Index (SI) is similar to the surface-based LI except that it is initially lifted from the 850 mb level. Convective Available Potential Energy (CAPE), is the most comprehensive stability index. It is the computed positive energy area on a Skew-t/Log P diagram. This index represents the amount of buoyant energy available to accelerate a parcel vertically.

Colman (1990a) found that elevated thunderstorms generally occur in a specific thermodynamic environment. Figure 9 (taken from Colman 1990a) shows the range of both surface and 850 mb-based LIs for which his elevated events occurred. Note that for most of his events, the surface-based air was stable, while at 850 mb, the mean instability was closer to neutral. The severe elevated convection which developed over southeast Indiana, developed in an area where surface-based LIs were forecast to be around +14 (Fig. 10a). Model-based SIs were forecast to be between +4 and +6 (Fig. 10b) in the vicinity of the March 23 convection, also quite stable. The Dayton, Ohio (DAY) sounding from 0000 UTC on March 23 (Fig. 11) indicated both an LI and SI of +15. Dayton is located in west-central Ohio, approximately 60 miles north of where the severe convection developed.

It was not until the 700 mb layer was lifted that only marginal instability became evident. Figure 12 shows the forecasted 700 mb-based LI ranging from +1 to -1 in the area covering east-central Illinois through northern Kentucky. The 0000 UTC DAY sounding indicated an unstable layer between 650 and 550 mb. Colman found that there was a lack of positive CAPE and generally a strong frontal inversion where elevated convection occurred. This was supported by the data observed from the 0000 UTC DAY sounding. Model gridded data also indicated a strong frontal inversion over this area. The "cap," which measures the ability of stable layers aloft to inhibit low-level parcel ascent was at 15°C, indicative of the environments' inability to initiate surface/low-level based convection (Graziano and Carlson 1987). CAPE values were forecast to be around 0 J/kg at 0000 UTC and then less than 100 J/kg at 0600 UTC. More importantly, model generated CAPE values over Tennessee were forecasted to be over 1000 J/kg. This corresponds well with the Memphis, TN sounding (not shown), which identified marginal to moderate instability (LI of -5 and CAPE value of 655 J/kg). This unstable air was the most likely source air for the elevated convection.

## 5. RADAR ANALYSIS

The KILN WSR-88D, which generate a variety of products (Klazura and Imy 1993), identified the development of convective cells over southeast Indiana and northern Kentucky. The first cells, which appeared in southeast Indiana shortly before 0430 UTC, had exhibited strengthening of the reflectivity returns in the mid-upper levels; correlating well with intensification of the storm's updraft. This was clearly observed in the Layered Composite Reflectivity Maximum

(LRM) product (not shown) where  $\geq 50$  dBZ reflectivity returns were indicated in the 24-33 kft MSL layer. Echo tops (max height of the 18.5 dBZ return) at this time were between 30-35 kft MSL, with low level reflectivity scans indicating 50-55 dBZ returns over Dearborn county in southeast Indiana. It was at this location that dime size hail was first reported. Just prior to the occurrence of this hail report, the Vertically Integrated Liquid Water (VIL) product, which has been found to be a good indicator of both small and large hail, had identified maximum values of 42-47 kg/m<sup>2</sup>; an apparent threshold that night for severe hail ( $\geq 0.75$ ").

Storm top divergence is also an indicator of the strength of a storm, and correlates well with the intensity of the updraft. Witt and Nelson (1991) investigated the relationship between a storm's divergent outflow magnitude at upper levels and maximum hailstone size by analyzing single-Doppler radar data for a number of events that occurred in Oklahoma during 1984 and 1985. The Storm-Relative Mean Radial Velocity Map (SRM) product is the product best used for determining divergence in the upper levels (or any level) of a storm. This product, by subtracting out the average motion of all identified storms, is used to detect shear regions (such as divergence signatures) that might be obscured by storm motion (Klazura and Imy 1993). At 0452 UTC, the storm which produced dime size hail exhibited a 52 kt divergent outflow signature at  $\approx 33$  kft MSL.

Shortly after 0500 UTC, storms began to develop over northern Kentucky. Movement of these storms was east-southeast, following the 850-500 mb quasi-geostrophic shear layer (Colman 1990b). Figure 1b depicts this steering profile. The strength of the most

intense storm was first noted in the LRM product at 0550 UTC (Fig. 13), where reflectivity values of  $\geq 57$  dBZ were observed above 24 kft MSL over Pendleton county Kentucky ( $\approx 40$  mi SSE of Cincinnati). The echo tops (maximum height of the 18.5 dBZ return) associated with this storm attained heights between 35-40 kft MSL, somewhat greater than the cells that produced the dime size hail earlier in southeast Indiana. Low level reflectivity images indicated that very intense returns were associated with this storm.

Figure 14, which depicts the lowest level reflectivity image at 0602 UTC, shows widespread convective activity across portions of southeast Indiana, southern Ohio, and northern Kentucky. The storm of interest was located at this time in southeast Pendleton county in Kentucky. It continued to move to the east-southeast, and was displaying a very strong 65 dBZ return. VILs for these storms were very similar to those earlier severe storms in southeast Indiana, with values ranging from 42-48 kg/m<sup>2</sup>. By 0608 UTC, this storm had moved to the east-southeast out of Pendleton county, and was now located in southern Bracken county Kentucky with an identified maximum VIL value of 48 kg/m<sup>2</sup> (Fig. 15).

For the severe storm that moved across portions of northern Kentucky during the period 0550-0613 UTC, divergent flow at upper levels ( $\approx 28$ -30 kft MSL) was consistently observed between 70-72 kts ( $\approx 20$  kts greater than the earlier severe storm that affected southeast Indiana). Figure 16 depicts this 72 kt divergent signature as it appeared over southern Bracken and western Robertson county Kentucky at 0608 UTC. This storm produced dime to golfball size hail as it crossed Pendleton, Bracken, Robertson and

Mason counties in Kentucky. In a study of severe elevated convection, Grant (1995) found that 92% of the severe weather reports associated with elevated convection were hail. This is due, in part, to cold air aloft that generally is in place when elevated convection is occurring.

## 6. SUMMARY

Elevated convection is difficult to forecast in that it occurs in spite of the existence of a stable surface environment. Past works by Colman (1984, 1990a and 1990b) have pointed to specific atmospheric conditions which would likely give rise to elevated convection. In this paper, the severe elevated convection that developed in the Ohio Valley on March 23, 1995 was assessed in light of this work performed by Colman. Both model gridded data, as well as local sounding data were analyzed in order to identify those mechanisms responsible for this convective development. Satellite imagery was used to track the history of these storms, while WSR-88D radar imagery allowed us to observe how the severe weather manifested itself in the storm scale.

According to climatic data, the Ohio Valley experiences a greater frequency of elevated convection than any points located longitudinally east of this area. The elevated convection that occurred on March 23 compared well with Colman's findings. Storms developed in a sector north to east-northeast of the surface low, and about 1.6 degrees latitude ( $\approx 95$  nm) north of a surface warm front. Extreme directional shear was also noted between the surface and 850 mb. At 850 mb, strong warm advection was present in a cyclonically curved flow ahead of the low level jet streak. Strong theta-e

advection was indicated as well at this level. Also consistent with Colman's findings was the observation of wind speeds increasing between the 850 and 500 mb levels.

Colman also found that the elevated convection occurs in an environment identified primarily by surface-based LIs greater than zero, and SIs (850 mb-based LIs) ranging between +10 and -10 (mean value near zero). The March 23 event fit well with these conditions. Another similarity between this case and those documented by Colman was the lack of any observed positive CAPE values.

For this event, instability became evident around the 700 mb level in the vicinity of where the convection developed, but with the source air probably coming from over Tennessee where surface-based CAPes averaged about 1000 J/kg. Radar imagery from the National Weather Service WSR-88D in Wilmington, OH showed the convective cells moving with the 850-500 mb layer quasi-geostrophic shear, and producing dime to golfball size hail.

#### ACKNOWLEDGEMENTS

Thanks go out to Gary Carter, Chief of the Scientific Services Division at the National Weather Service Eastern Region Headquarters, for the critical review of this paper. Also, thanks to the personnel at both NCDC and NESDIS who provided valuable data for this study.

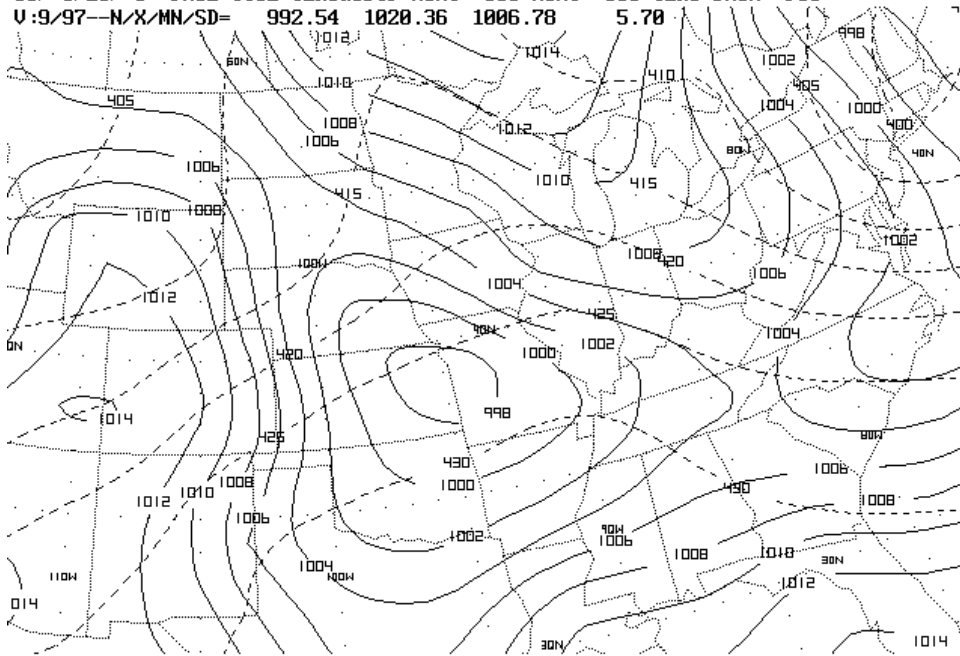
#### REFERENCES

- Colman, B. R., 1984: Deep convection occurring above a stable planetary boundary layer. Sc.D. Dissertation, Massachusetts Institute of Technology, 243 pp.
- \_\_\_\_\_, 1990a: Thunderstorms above frontal surfaces in environments without positive CAPE. Part I: A climatology. *Mon. Wea. Rev.*, **118**, 1103-1121.
- \_\_\_\_\_, 1990b: Thunderstorms above frontal surfaces in environments without positive CAPE. Part II: Organization and instability mechanisms. *Mon. Wea. Rev.*, **118**, 1123-1144.
- Grant, B. N., 1995: Elevated cold-sector severe thunderstorms: A preliminary study. *Nat. Wea. Dig.*, **19**, 25-31.
- Graziano, T. M., and T. N. Carlson, 1987: A statistical evaluation of lid strength on deep convection. *Wea. Forecasting*, **2**, 127-139.
- Hart, J. A., and W. D. Korotky, 1991. The SHARP Workstation v1.50. A skew T/hodograph analysis and research program for the IBM and compatible PC. User's Manual. NOAA/NWS Forecast Office, Charleston, WV, 62 pp.
- Klazura, G. E., and D. A. Imy, 1993: A description of the initial set of analysis products available from the NEXRAD WSR-88D system. *Bull. Amer. Meteor. Soc.*, **7**, 1293-1311.

National Weather Service, 1991: Federal Meteorological Handbook No. 11. Doppler Radar and Meteorological Observations. Part A: System concepts, responsibilities, and procedures, 21 pp.

Witt, A., and S. P. Nelson, 1991: The use of single-Doppler radar for estimating maximum hailstone size. *J. Appl. Meteor.*, **30**, 425-431.

ETAX:LVL= 500:LVR=1000/ 500 :FHR= 0:FHRS= 0/ 24::FIL2= MR239500.ETS  
 95/ 3/23/ 0--PMSL CI02 CLR3&SDIF HGHT 500 HGHT 850 CLR3 DASH F00  
 U:9/97--N/X/MN/SD= 992.54 1020.36 1006.78 5.70



ETAX:LVL= 500:LVR=1000/ 500 :FHR= 6:FHRS= 0/ 24::FIL2= MR239500.ETS  
 95/ 3/23/ 0--PMSL CI02 CLR3&SDIF HGHT 500 HGHT 850 CLR3 DASH F06  
 U:9/97--N/X/MN/SD= 993.88 1021.36 1008.84 5.51

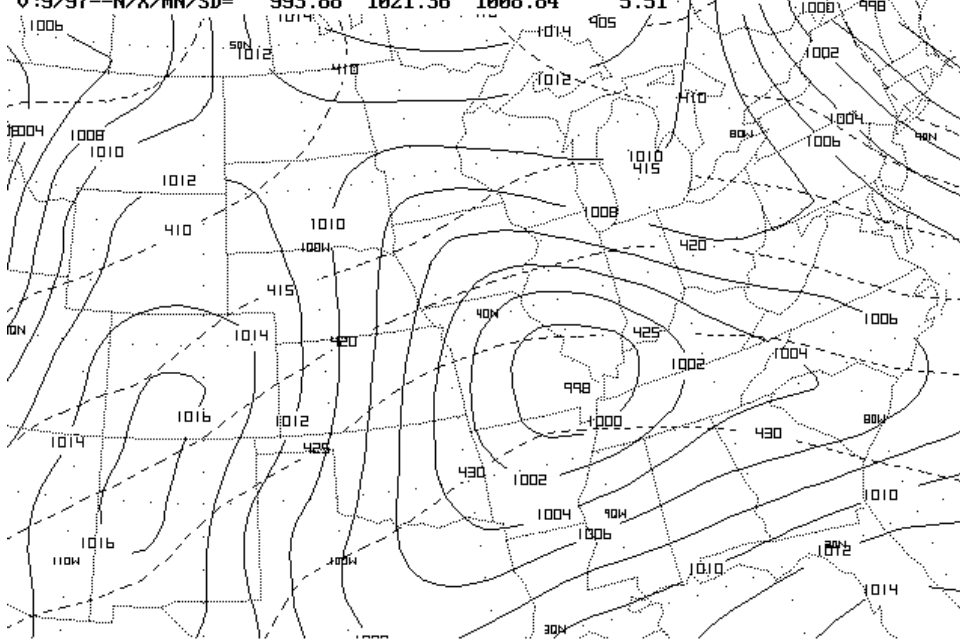


**Figure 1a and 1b.** ETA model 0000 UTC analysis (top) and 6-hr forecast (bottom) of surface pressure and 850-500 mb thickness from March 23, 1995. Thickness lines are dashed and are in dm. Solid lines are surface pressure in mb.



ETAX:LVL= 850:LVR=1000/ 500 :FHR= 6:FHRS= 0/ 24::FIL2= MR239500.ETS  
 95/ 3/23/ 0--PMSL C102 CLR3&BKNT 850 CLR3 F06  
 U:9/97--N/X/MN/SD= 993.88 1021.36 1008.84 5.51

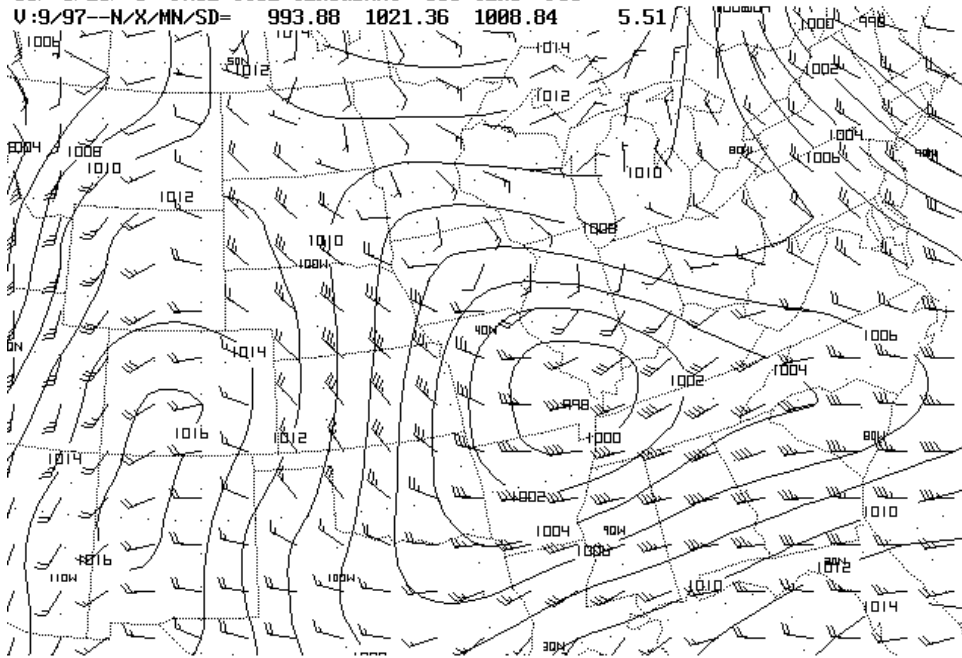


**Figure 2.** 6-hr forecast of surface pressure (mb) and 850 mb wind barbs (kts) from the 0000 UTC ETA model on March 23, 1995.

ETAX:LVL= 850:LVR=1000/ 500 :FHR= 6:FHRS= 0/ 24::FIL2= MR239500.ETS  
 95/ 3/23/ 0--BKNT GT20 CLR3&ADVT TEMP WIND GT00 DASH CLR3&HGHT C110 CLR3  
 U:9/97--N/X/MN/SD= .51 44.10 15.94 24.86

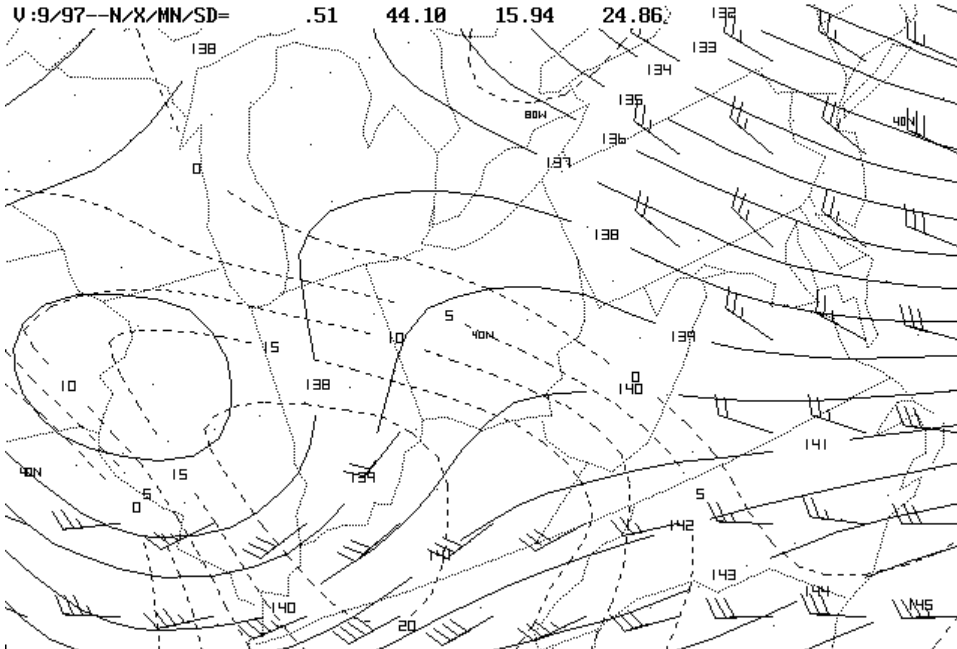


**Figure 3.** 6-hr forecast of 850 mb heights (solid line), warm advection (dashed) and winds >20 kts from the 0000 UTC ETA model on March 23, 1995.

ETAX:LVL= 850:LVR=1000/ 500 :FHR= 6:FHRS= 0/ 24::FIL2= MR239500.ETS  
 95/ 3/23/ 0--ADVT THIE WIND GT00 850 CLR3  
 U:9/97--N/X/MN/SD=-7.40E-04 7.69E-04-3.07E-05 2.04E-04

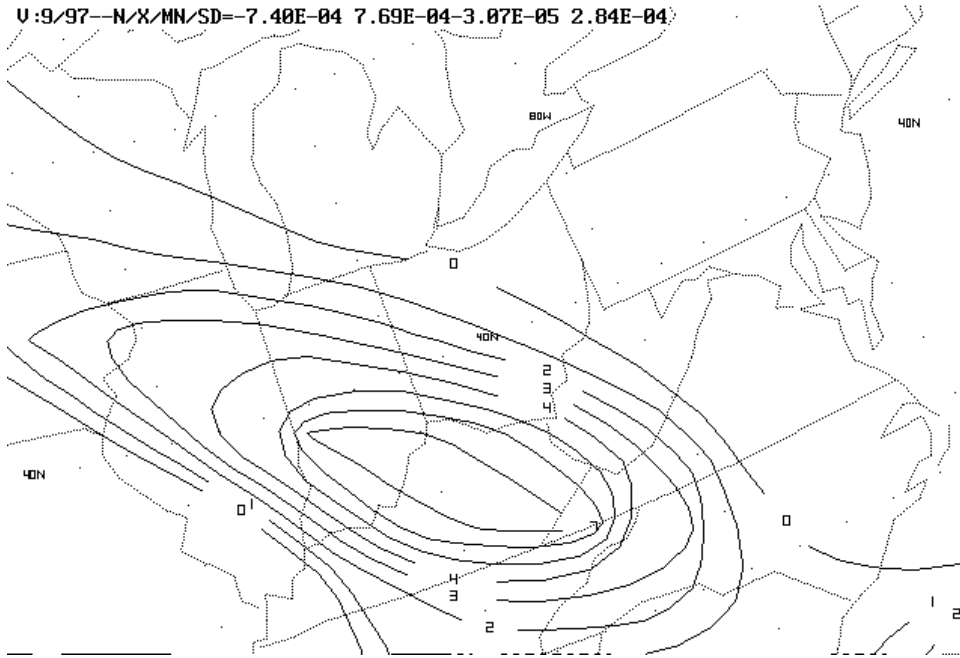


**Figure 4.** Analysis of positive 850 mb theta-e advection from the 0000 UTC ETA model on March 23, 1995.

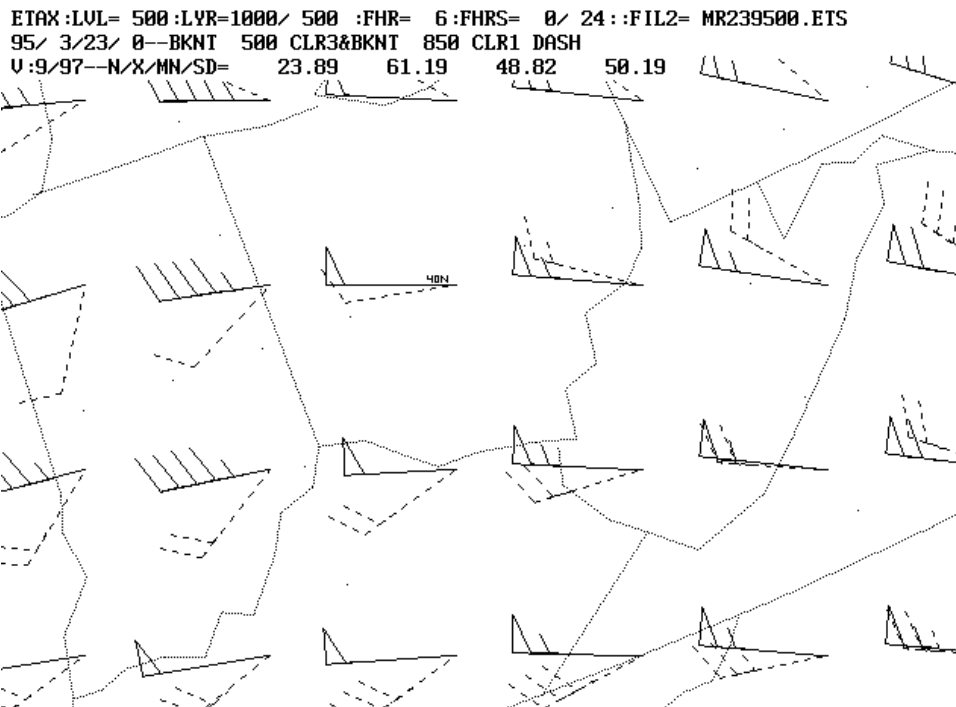
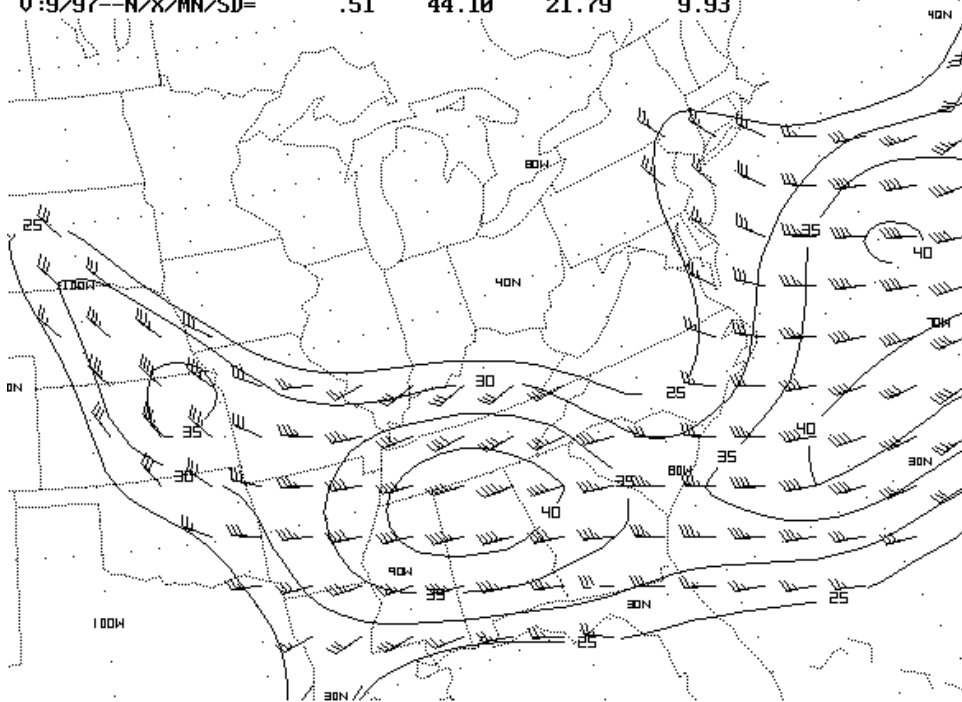


**Figure 5.** 6-hr forecast of 500 (dark) and 850 (light) mb winds (kts) from the 0000 UTC ETA model on March 23, 1995.

ETAX:LVL= 850:LVR=1000/ 500 :FHR= 6:FHRS= 0/ 24::FIL2= MR239500.ETS  
 95/ 3/23/ 0--WSPK GT25 CI05 CLR3&BKNT GT25 CLR3 850  
 U:9/97--N/X/MN/SD= .51 44.10 21.79 9.93



ETAX:LVL= 500:LVR=1000/ 500 :FHR= 6:FHRS= 0/ 24::FIL2= MR239500.ETS  
 95/ 3/23/ 0--WSPK GT45 CI05 CLR3&BKNT GT50 CLR3 500  
 U:9/97--N/X/MN/SD= 5.28 76.92 38.65 16.20

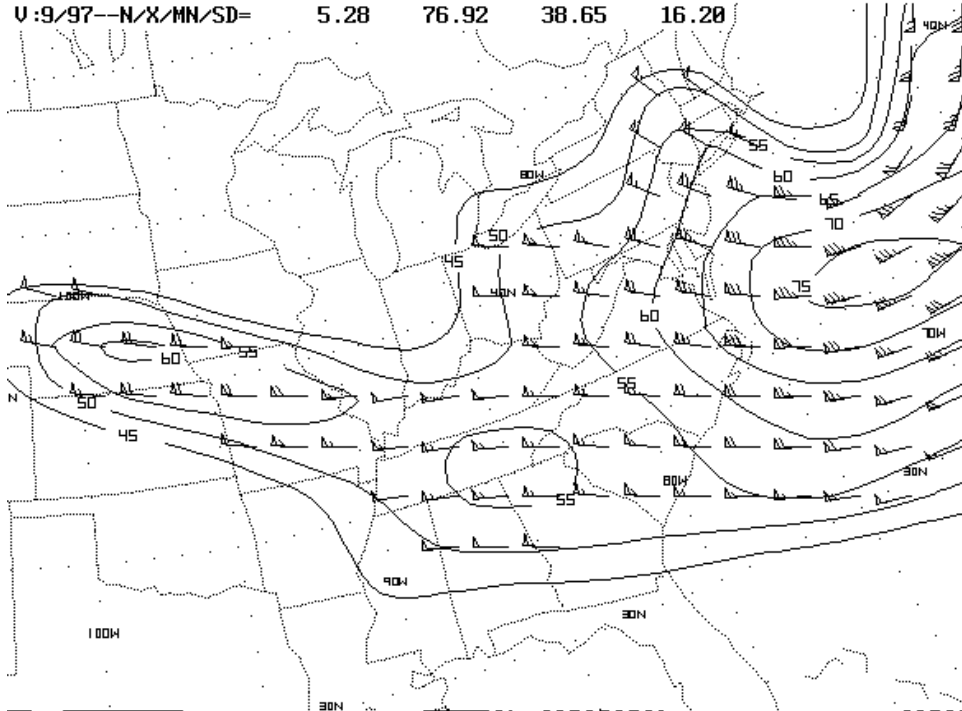


**Figure 6a and 6b.** 6-hr forecast of 850 mb (top) and 500 mb (bottom) wind speeds (kts) from the 0000 UTC ETA model on March 23, 1995.

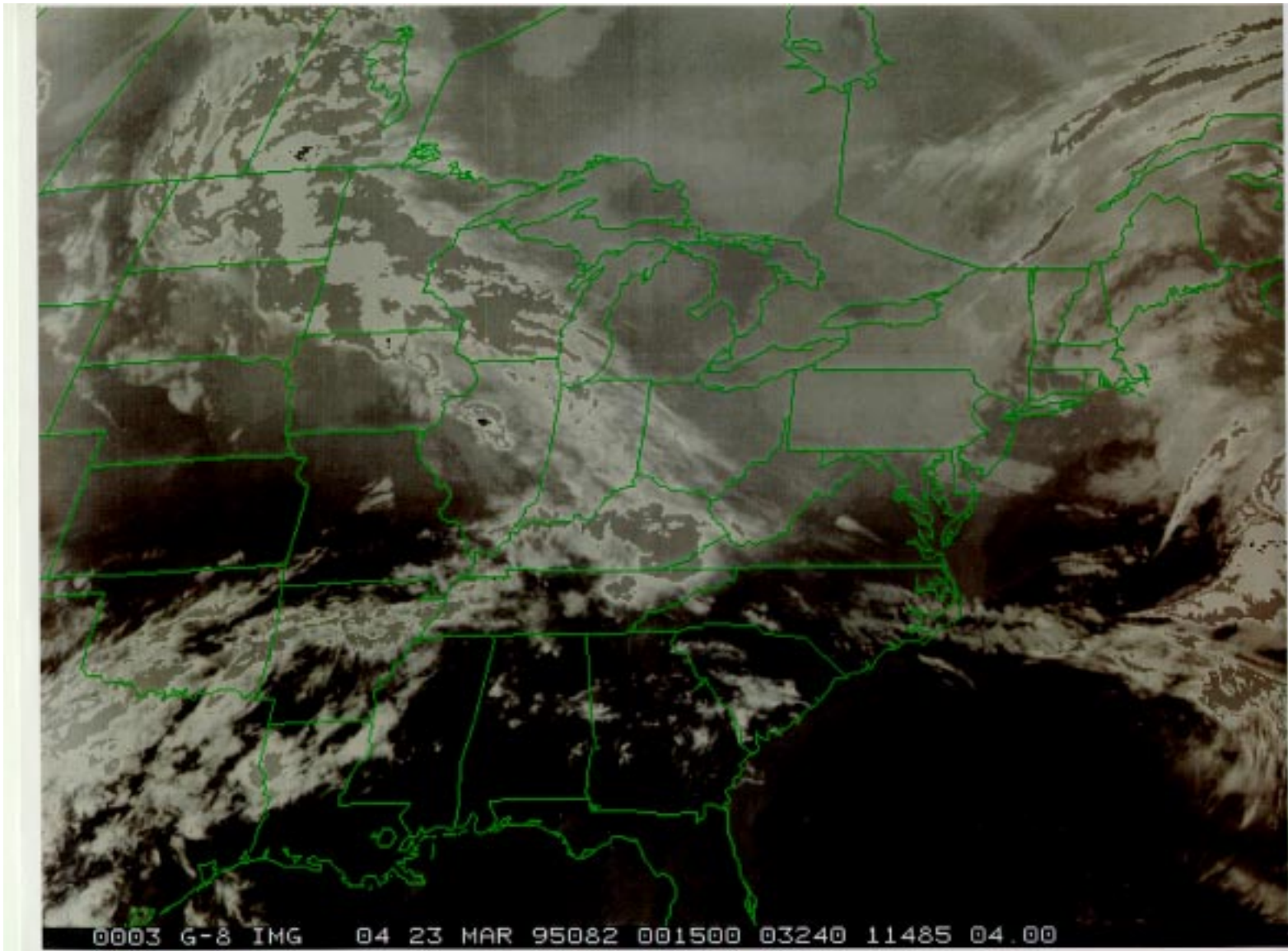


**Figure 7.** Infrared satellite image for 0015 UTC on March 23, 1995.

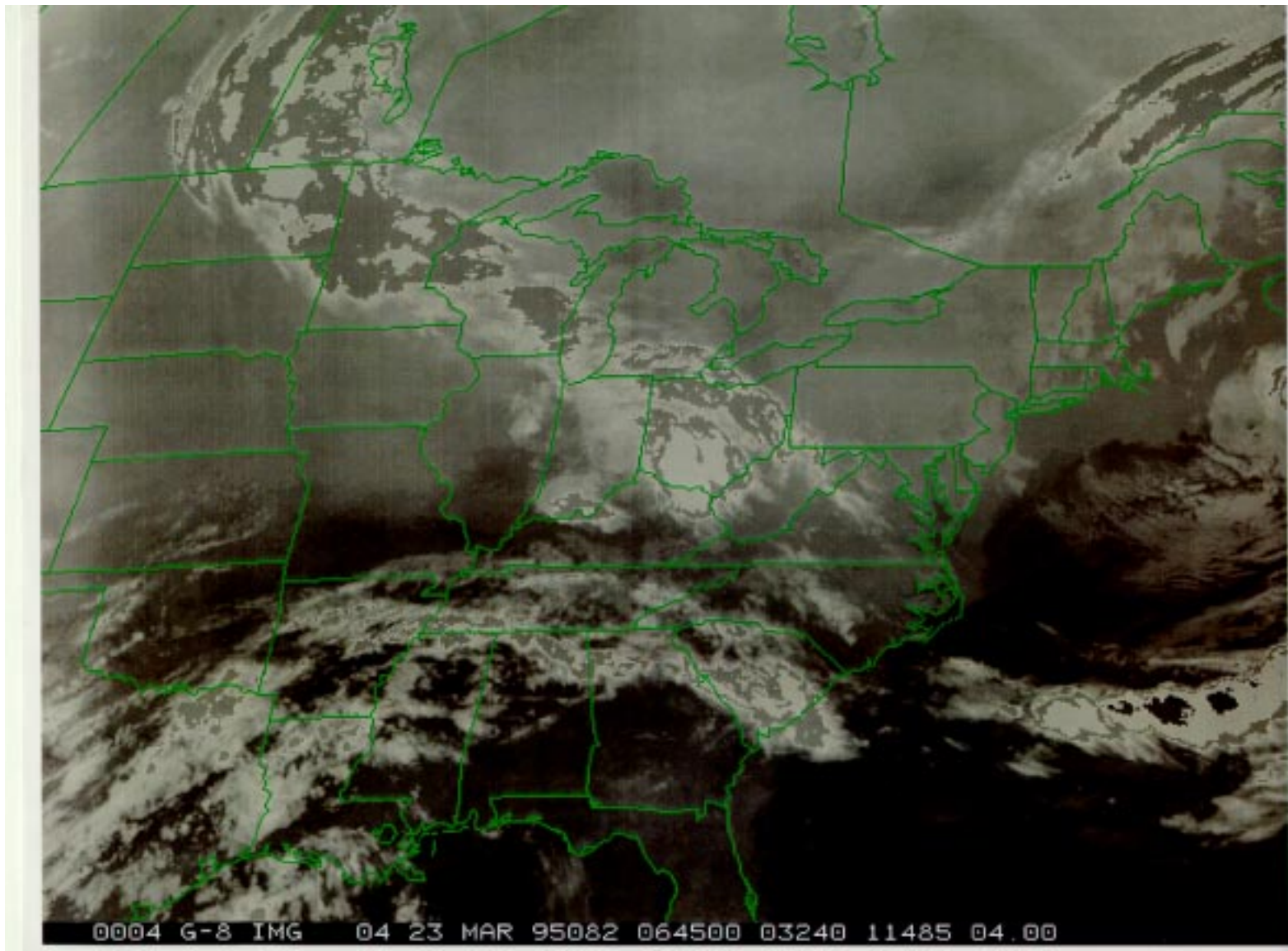


**Figure 8.** Infrared satellite image for 0645 UTC on March 23, 1995.

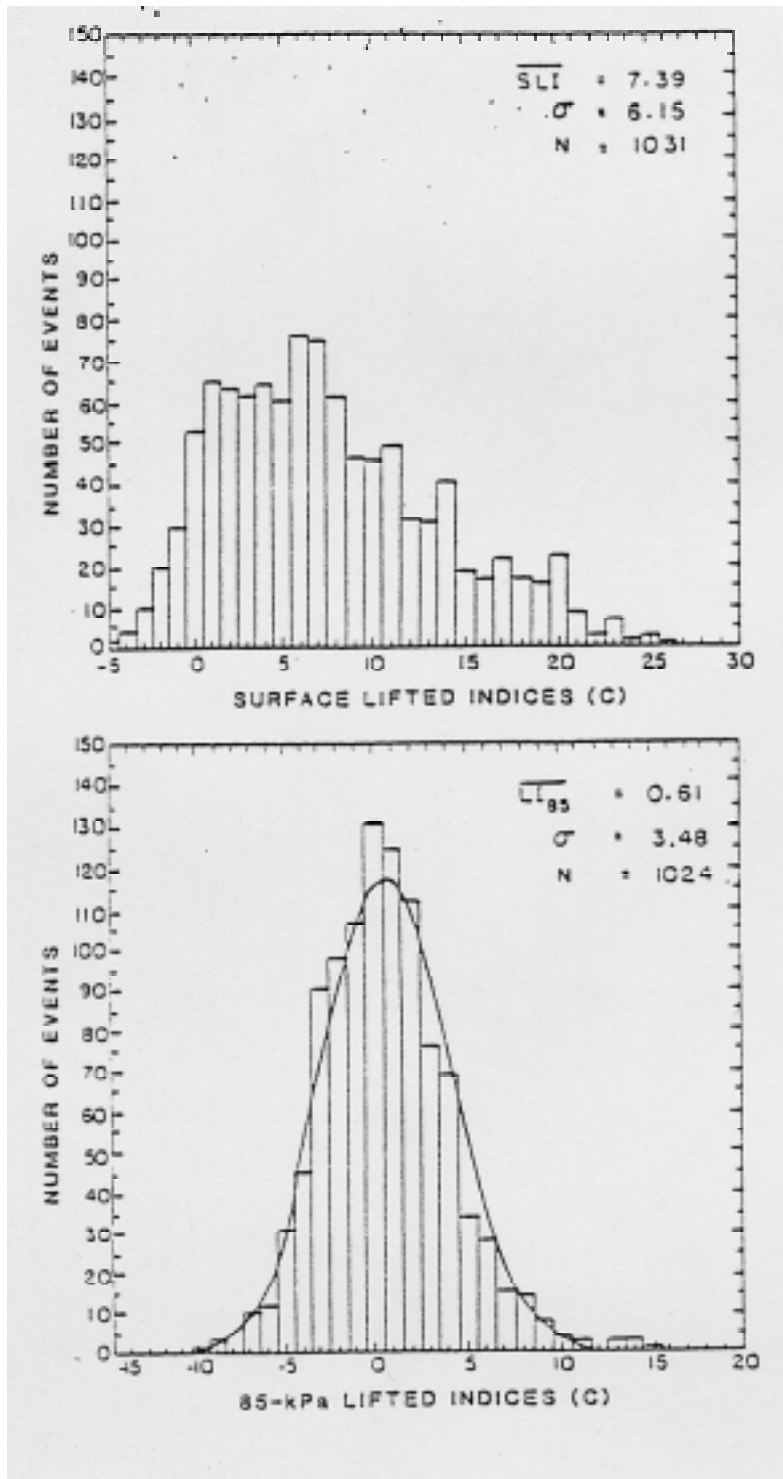
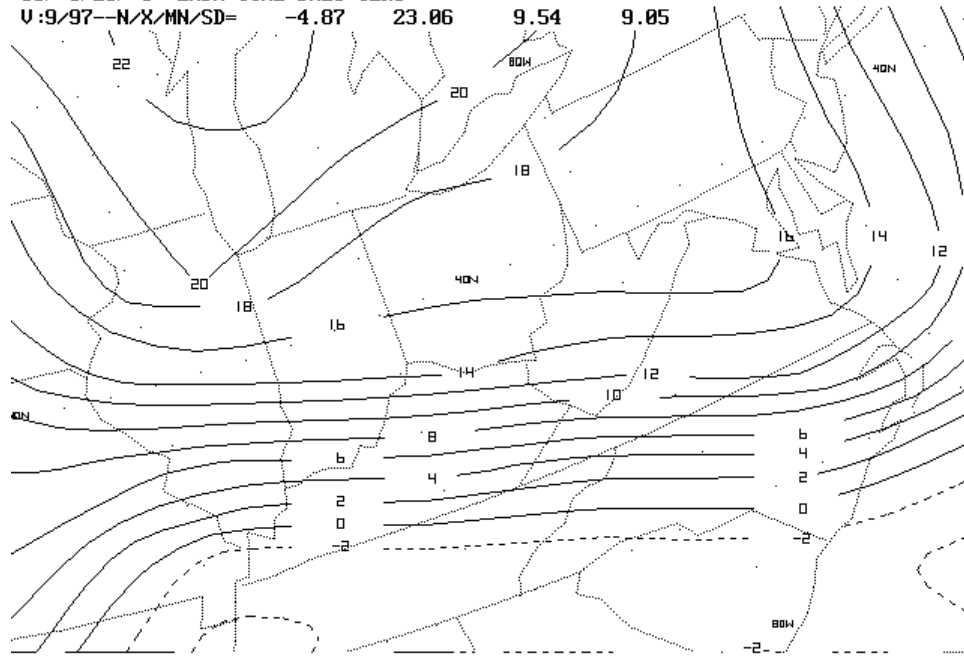


**Figure 9.** (taken from Colman 1990a) Histograms of the surface and 850 mb Lifted Indices (°C) for elevated thunderstorm events used in Colman's 4-year study.

ETAX:LVL=1000:LYR=1000/ 500 :FHR= 6:FHRS= 0/ 24::FIL2= MR239500.ETS  
 95/ 3/23/ 0—LNDX CIN2 DNEG CLR3  
 U:9/97—N/X/MN/SD= -4.87 23.06 9.54 9.85



ETAX:LVL= 850:LYR=1000/ 500 :FHR= 6:FHRS= 0/ 24::FIL2= MR239500.ETS  
 95/ 3/23/ 0—LNDX CIN2 DNEG CLR3  
 U:9/97—N/X/MN/SD= -2.98 18.53 8.44 6.55

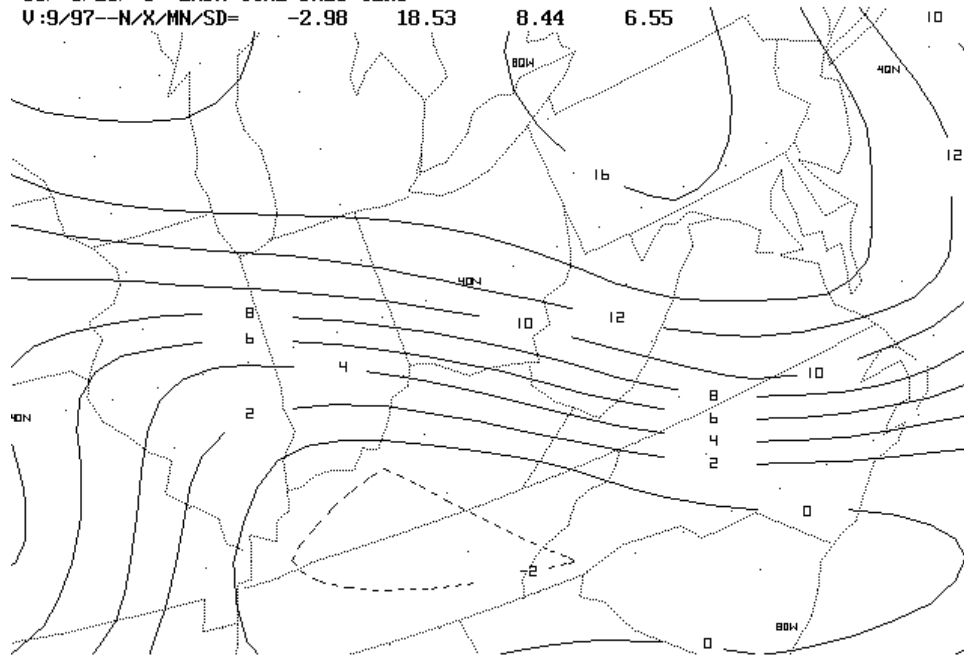


**Figure 10a and 10b.** 6-hr forecast of surface-based LIs (top) and Showalter Index (bottom) from the 0000 UTC ETA model on March 23, 1995. Negative values are dashed.





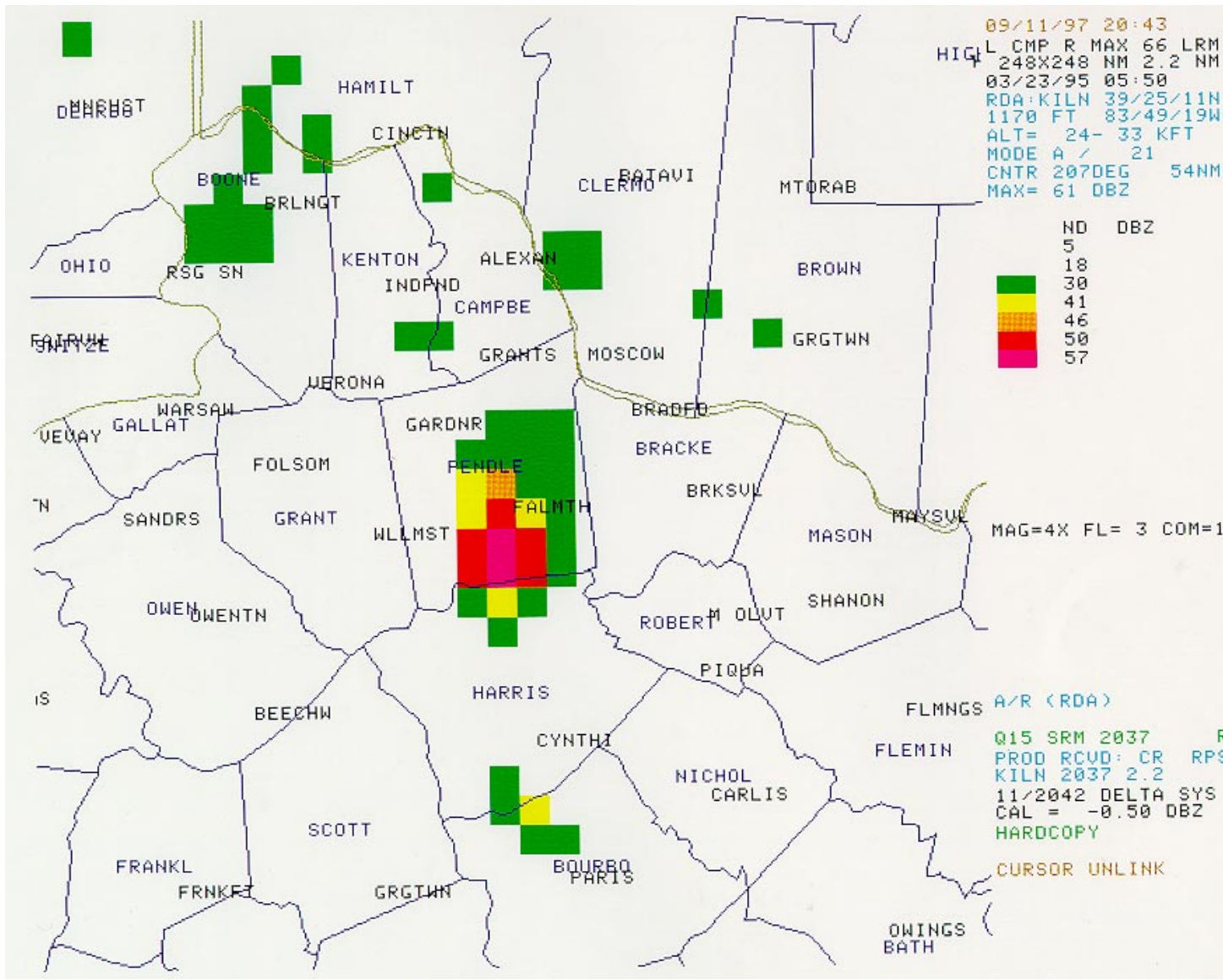


**Figure 13.** Wilmington, Ohio WSR-88D Layer Composite Reflectivity Maximum product (24-33 kft layer) at 0550 UTC on March 23, 1995. Data filtered below 30 dBZ.

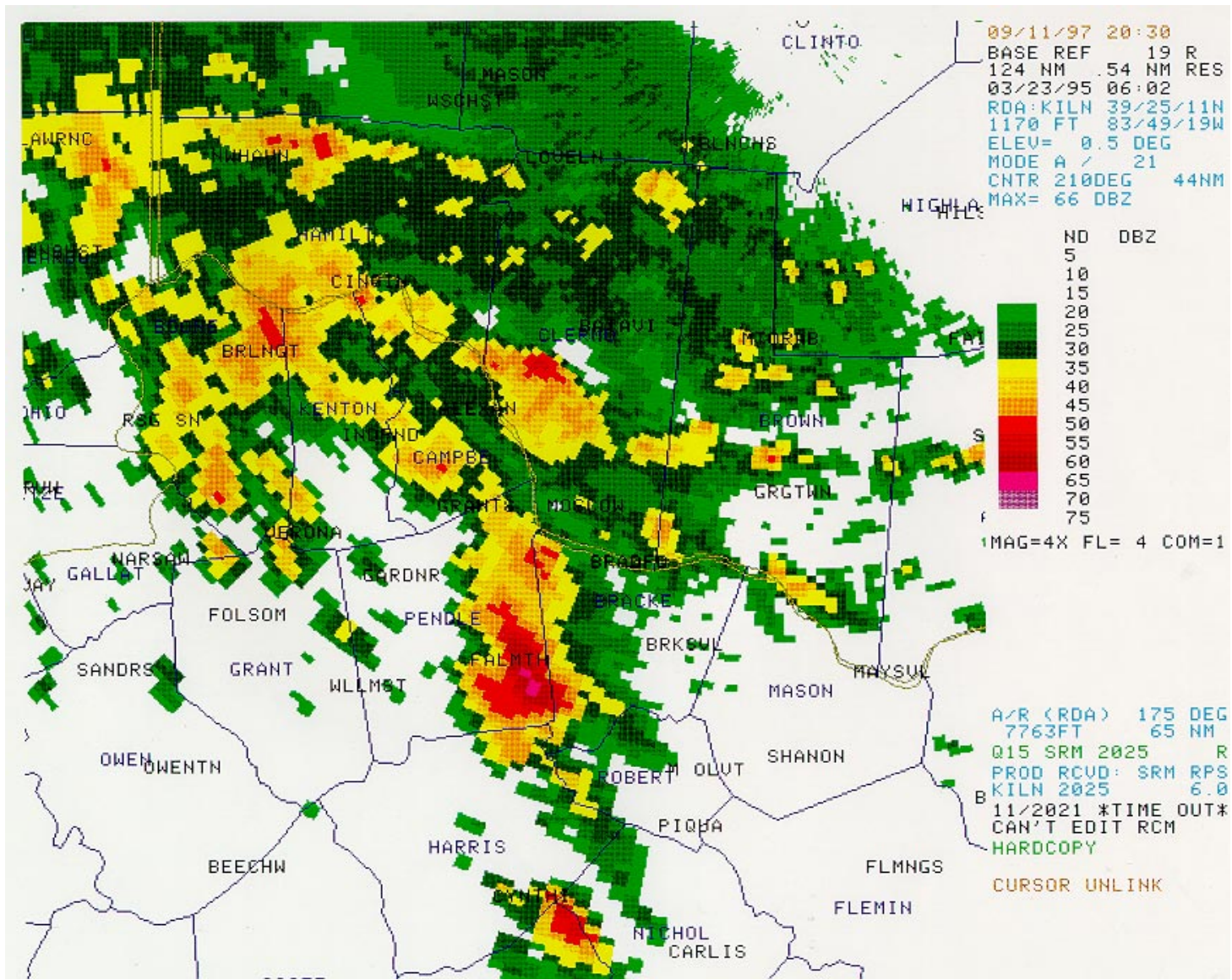
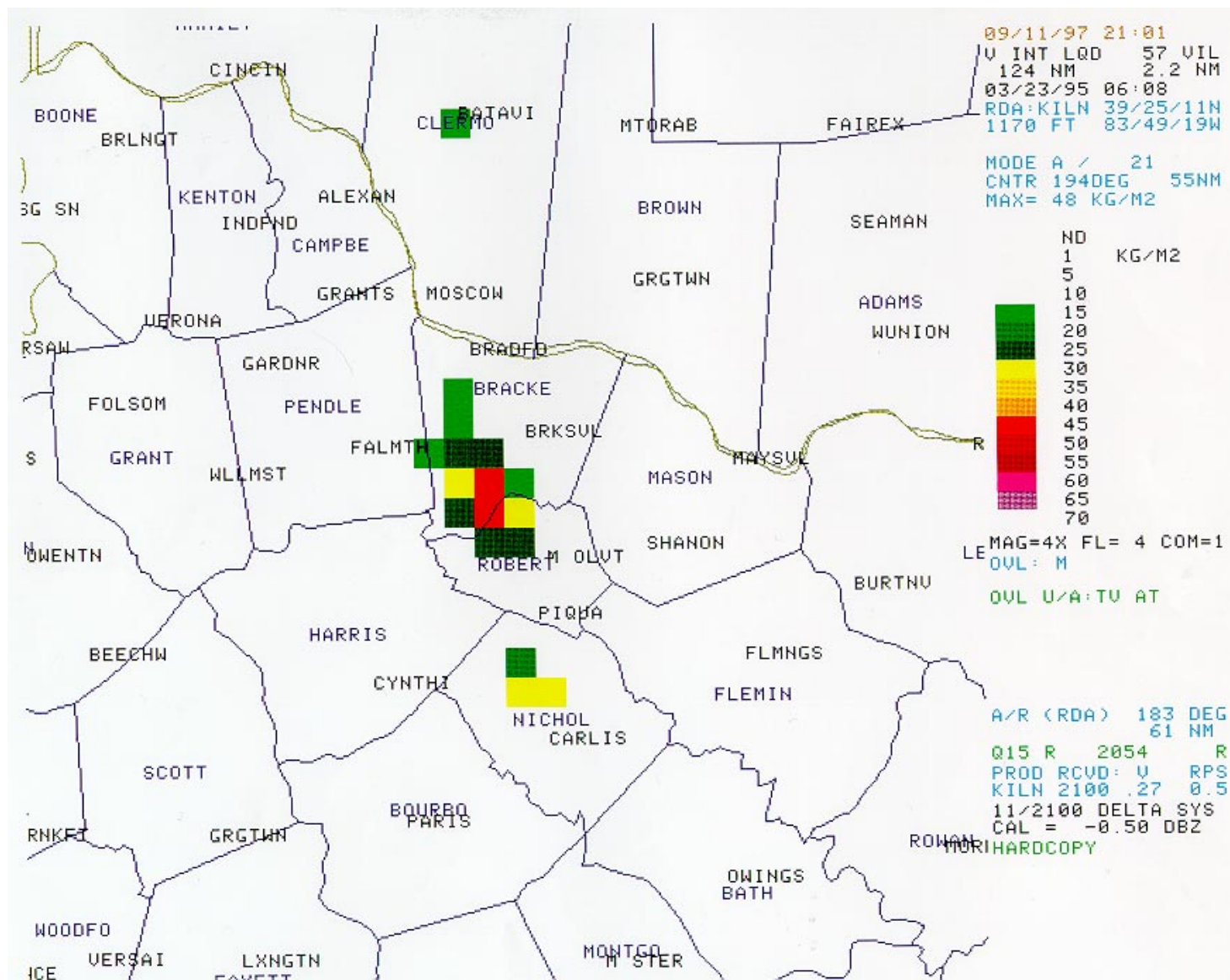
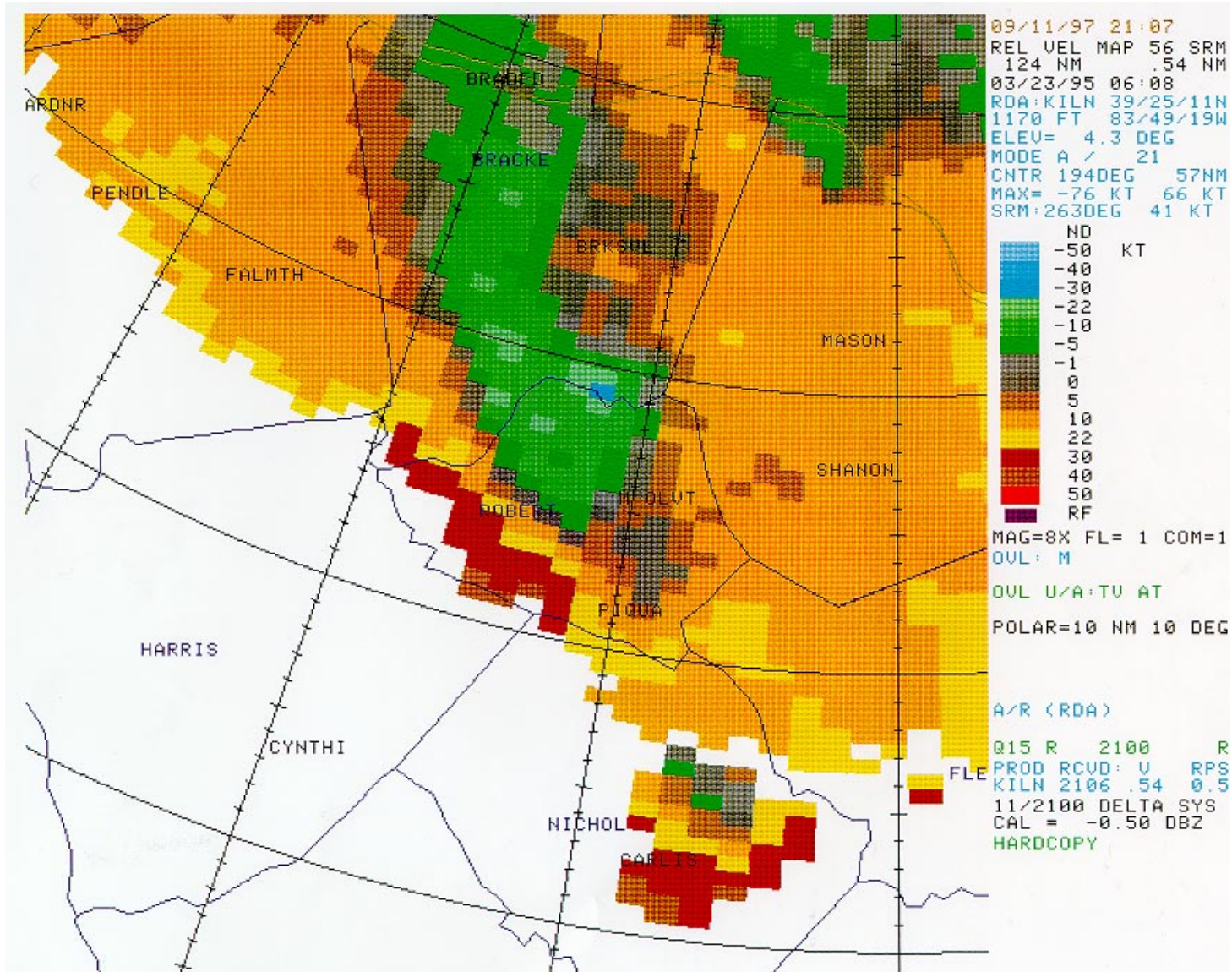


Figure 14. Wilmington, Ohio WSR-88D Base Reflectivity product from the 0.5° elevation angle at 0602 UTC on March 23, 1995. Data filtered below 20 dBZ.



**Figure 15.** Wilmington, Ohio WSR-88D Vertically Integrated Liquid Water product at 0608 UTC on March 23, 1995. Data filtered below the value of 15 kg/m<sup>2</sup>.



**Figure 16.** Wilmington, Ohio WSR-88D Storm Relative Mean Radial Velocity Map from the 4.3° elevation angle scan at 0608 UTC on March 23, 1995. Strong divergence signature located at center of image.